# Influence of the Insulation Defects Size on the Value of the Wire Capacitance


**Galina Vavilova, Vladislav Yurchenko, and Li Keyan**

**Abstract** The study focuses on detection of defects in the single-core electrical wire insulation by changing the linear capacity of the electric wire. Numerical simulation was performed to create defects that are difficult to implement in practice. In the study, models of the following defects were created: local thinning of the wire insulation, eccentricity, foreign inclusion in the wire insulation. During the study, the depth and length of the 'local thinning' defect in the wire insulation, the shift of the core center relative to wire the center, length and thickness of the 'foreign inclusion' defect were varied. As a result, absolute and relative values of the geometric dimensions of the defects that cause a significant change in the wire capacitance are revealed. A significant deviation of the capacitance is taken at the level of 5% deviation from the nominal value of the capacitance of a defect-free wire in accordance with the requirements of normative and technical documentation and the accuracy of device for in-process testing of the wire capacitance. The paper reports the results of the initial study. Further research is required to increase the reliability of the models used.

G. Vavilova (✉)
Division for Testing and Diagnostics, National Research Tomsk Polytechnic University, 30 Lenin Avenue, Tomsk, Russia 634050
e-mail: wgw@tpu.ru

V. Yurchenko
Department of Information Technology and Security, Karaganda Technical University, 56 Ave. Nursultan Nazarbayev, Karaganda 100027, Republic of Kazakhstan
e-mail: jurchenkovv@mail.ru

L. Keyan
Inspection Business Department, National Lighting Test Center, No. 3 A, Dabeiyaochangpo Village, Chaoyang District, Beijing 100020, China
e-mail: 393678364@qq.com

© The Author(s), under exclusive license to Springer Nature Switzerland AG 2021

I. V. Minin et al. (eds.), *Progress in Material Science and Engineering*,
Studies in Systems, Decision and Control 351,
https://doi.org/10.1007/978-3-030-68103-6_11

## 1 Introduction

Electrical wires are widely used in various industries. The wire quality has a direct impact on the quality and safety of the products in which it is used. In the minimum optional, a simple single-core wire is a metal core and polymer insulation applied over it [1–3].

The main indicator of the wire quality is the absence of defects in its design [4]. A defect is understood as any nonconformity of a product with established requirements [5, 6].

The presence of any even minor defect causes deviation from its nominal geometric and electrical parameters. At the production stage, an electric wire can include various types of defects [6–8]: local thinning or increased outer diameter of the insulation, foreign inclusions in the insulation, porous insulation, eccentricity, etc.

In wire manufacturing [9], defects should be detected at the yearly stage in order to timely improve the technological process, which will reduce the economic costs of cable product manufacturing. During the technological process, defects can be detected through the change in the linear capacity of the wire [7, 8, 10, 11].

The study of the effect of the geometric parameters of different defects on other parameters of electrical wires will allow their timely in-situ detection. The aim of the study is to determine geometric dimensions of insulation defects, which significantly impact the change in the electric wire linear capacity.

## 2 Wire Model

A detailed study of wire samples with different types of defects of different sizes. A number of reasons hampers creation of the bank of wire samples:

- resources are required to create an extensive bank of wire samples with defects;
- not all types of defects can be created artificially, in particular to ensure the variability of the geometric parameters of defects.

These problems can be partially solved through modeling [12–14], which reduces the cost of creating a large volume of real samples with different geometric dimensions of defects and simultaneously increases the study efficiency due to a variety of models of defects of various types and sizes [13].

A single-core wire can be regarded as a cylindrical capacitor (Fig. 1), which consists of a metal core diameter $d$ and polymer insulation diameter $D$ [15]. The core surface is considered as the first capacitor plate. Voltage is applied to the outer surface of the insulation, and this boundary is considered as the second capacitor plate. The inter-plate space is filled with dielectric, which is the insulation material of the wire [16, 17].

The capacity of the capacitor can be calculated using a well-known equation [18]:

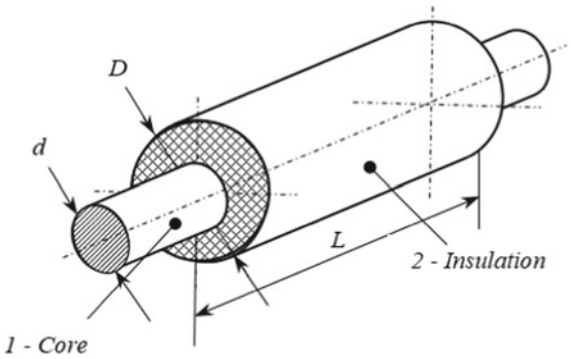


**Fig. 1** Model and appearance of the wire

$$C = \frac{2\pi \cdot \varepsilon \cdot \varepsilon_0 \cdot L}{\ln\left(\frac{D}{d}\right)}, \tag{1}$$

The research object f is a mathematical model of a single-core wire with a core diameter $D = 1$ mm and an insulation diameter $d = 3$ mm. The wire insulation is polyethylene with dielectric constant $\varepsilon = 2.3$. The wire model length is equal to the length of the measuring electrode of the device for in-process testing of the wire capacitance ($L = 20$ cm) [9, 10, 18].

The capacitance of a defect-free wire of the specified dimensions is $C = 23.28$ pF. This value is taken as nominal.

## 3 Insulation Defects

Defects change geometric dimensions of the wire, and hence, they affect the capacitance value. The deviation of the capacitance in the presence of a defect is recorded relative to the nominal value—the capacitance of the defect-free wire. In accordance with the requirements of normative and technical documentation [19–22] and the accuracy of device for in-process testing of the wire capacitance [9, 10, 18], a significant change in the capacitance is taken at the level of 5% of the deviation from the nominal capacitance of the defect-free wire, which corresponds to $C_1 = 21.85$ pF and $C_2 = 24.15$ pF.

The types of defects modeled in the study are as follows:

- local thinning of the wire insulation (external defect);
- eccentricity (displacement of the core center from the wire center);
- foreign inclusion in wire insulation (intrinsic defect).

### 3.1 Local Thinning of the Wire Insulation

Figure 2 shows a defect model—local thinning of the wire insulation. The defect depth is determined by the $2h_x$ change in the insulation outer diameter $D$ in the defect area. In the defect area, the insulation diameter is $D_d = D - 2h_x$.

In the presence of this defect, the sample can be divided into 3 sections: two sections of length $L_1$ and $L_2$ with the initial insulation diameter $D$ and one section of length $l_x$ with a smaller insulation diameter $D_d$. To simplify calculations, the defect boundaries are assumed sharp.

The capacity for each section is calculated by Eq. (1) separately, with regard to the geometric dimensions of each section. The capacity value for each section is indicated $C_{sec1}$, $C_{sec2}$ and $C_{sec3}$, respectively (Fig. 2).

The total length of all wire sections corresponds to the total length ($L = 20$ cm) of the wire sample.

The general equation for calculating the wire capacity takes the form:

$$C = \frac{2\pi \cdot \varepsilon_0 \cdot \varepsilon \cdot (L_1 + L_2)}{\ln\left(\frac{D}{d}\right)} + \frac{2\pi \cdot \varepsilon_0 \cdot \varepsilon \cdot l_x}{\ln\left(\frac{D_d}{d}\right)} \tag{2}$$

Numerical modeling was used to carry out the studies.

Figure 3a shows dependence of the wire capacitance with the *local thinning of the wire insulation* on changes in the defect length in the range from 0 to 5 cm at constant depth $hx = 0.5$ mm. Figure 3b shows dependence of the relative error in the changed wire capacitance on relative changes in the volume of the defective wire. To compare the results of the study, the concept of *the wire nominal volume* should be introduced, which corresponds to the insulation volume of the non-defective wire. The nominal volume of the wire is calculated using the formula for the volume of the cylinder, with regard to the geometric dimensions of the core and wire insulation. The considered defects cause a decrease in the insulation volume.

In Fig. 3a, b, the horizontal line indicates the capacitance corresponding to the threshold value in the absolute and relative form (deviation ±5%), which can be observed in all the graphs given below.

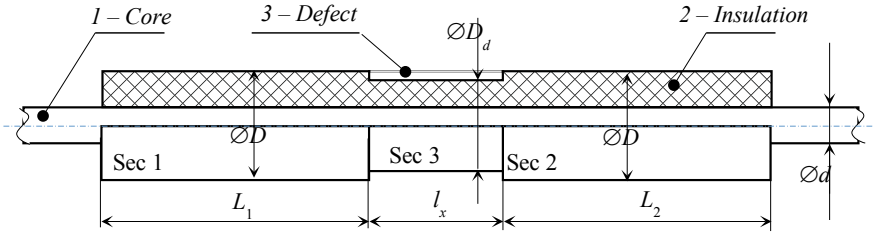


**Fig. 2** Model of the defect Local thinning of the wire insulation

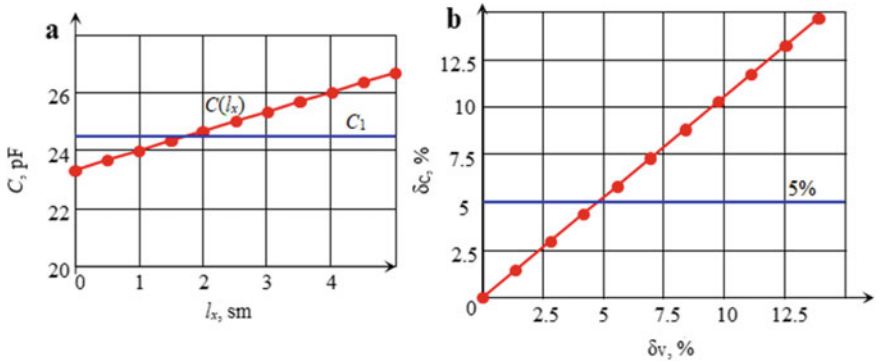


**Fig. 3** Change in wire capacity **a** and relative error **b** in the presence of local length of the diameter (constant depth defect)

The defect *Local thinning of the diameter* increases the capacitance (Fig. 3). It should be noted that wire capacitance changes significantly when the defect length attains $l_x = 18$ mm and the volume of the wire insulation decreases by more than 4.5%.

Figure 4a shows dependence of the wire capacitance on changes in the defect depth in the range from 0 to 0.9 mm at constant length $l_x = 10$ mm. Figure 4b shows dependence of the relative error of the wire capacitance on relative changes in the volume of the wire insulation.

Figure 4 shows that wire capacitance changes significantly at defect depth $hx = 0.65$ mm, which corresponds to changes in the wire volume by more than 3.3%.

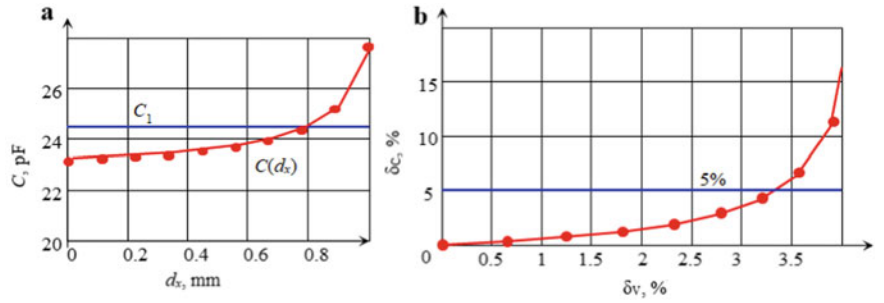


**Fig. 4** Change in wire capacity **a** and relative error **b** in the presence of local thinning of the diameter (constant length defect)

### 3.2 *Eccentricity*

Eccentricity is deviation of the core center from the wire center [23, 24]. Figure 5 shows the *eccentricity* model and a graphical diagram for capacitance calculation.

Based on Eq. (1) and mathematical analysis [25–27] of data from Fig. 5b, the equation can be derived for dependence of the capacitance on the core displacement relative to the wire center:

$$C(m) = \frac{2\pi \cdot \varepsilon \cdot \varepsilon_0 \cdot l}{\ln\left(\frac{H_2 R}{H_1(m) \cdot r}\right)} \tag{2}$$

where $r = d/2$, $R = D/2$ are the core and insulation radii, mm; $m$ is eccentricity, mm; $H1$,$H2$ are the distance from the axis to the center of the core and wire, respectively, mm (the selected point is on the insulation surface).

If we assume that $H_2 = R$, then $H1(m) = R - m$.

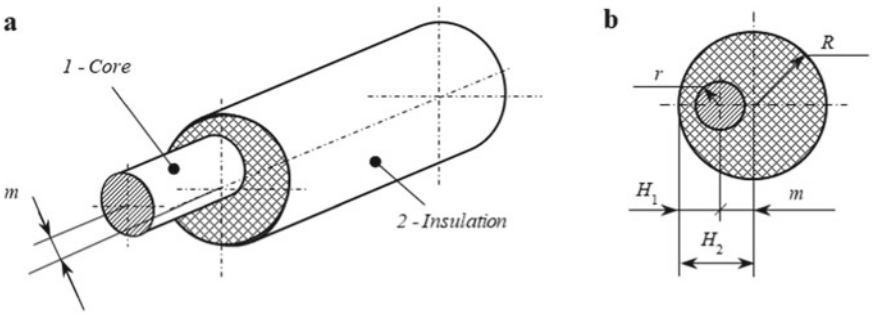


**Fig. 5** Wire eccentricity: **a** general view, **b** incision

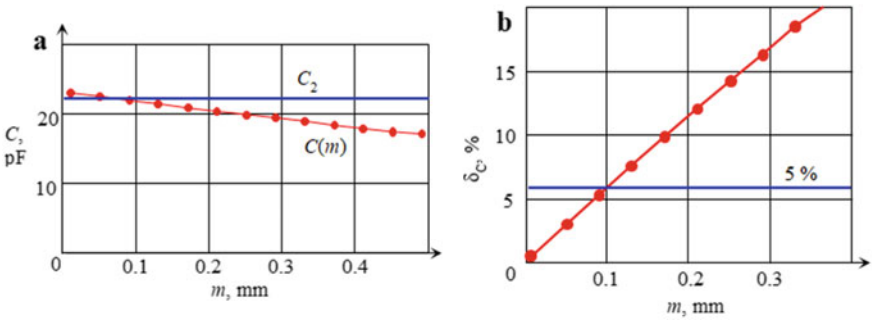


**Fig. 6** Change in wire capacitance **a** and relative error **b** on wire eccentricity

Figure 6a shows dependence of the wire capacitance on the core displacement relative to the wire center $m$ in the range from 0 to 0.5 mm. Figure 6b shows dependence of the relative error of the wire capacitance on the core displacement.

Figure 6 shows that eccentricity leads to a decrease in the wire capacitance. The threshold value of the wire capacitance is exceeded if eccentricity is more than 0.1 mm, which corresponds to 10% of the core diameter.

## 3.3 Foreign Inclusion

Figure 7 shows the *Foreign inclusion in wire insulation* model. Foreign inclusion is the presence of an air bubble, metal shavings or other object in the homogeneous structure of insulation [24, 27]. For ease of modeling, a section is taken inside the insulation along the entire circumference. The defect size is determined by the length $l_x$ and the diameter of the defect inner $D_2$ and outer $D_3$ surfaces. The case is considered when the inner space of the defect is filled with air with a dielectric constant $\varepsilon_1 = 1$.

The wire capacitance of this defect can be calculated using a classical formula for a cylindrical capacitor (Eq. 1) with regard to recommendations provided in [28–30]. In this case, the wire sample capacity is calculated as the sum of capacities for each of the three sections (similar to *Local thinning of the wire insulation*). Section 2 is considered to be a multilayer cylindrical capacitor [30, 31], which comprises 3 insulation layers of known thickness: polyethylene—air—polyethylene. After conversion, the formula for calculating the capacity has the form:

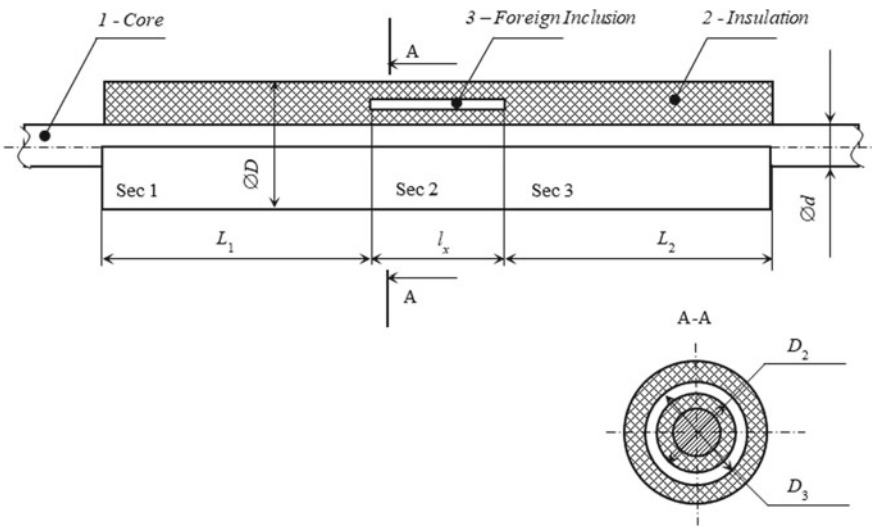


**Fig. 7** Model of the *Foreign inclusion* defect

$$C = \frac{2\pi \cdot \varepsilon_0 \cdot (L_1 + L_2)}{\frac{1}{\varepsilon} \ln\left(\frac{D}{d}\right)} + \frac{2\pi \cdot \varepsilon_0 \cdot l_x}{\frac{1}{\varepsilon}\left(\ln\left(\frac{D_2}{d}\right) + \ln\left(\frac{D}{D_3}\right)\right) + \frac{1}{\varepsilon_1} \ln\left(\frac{D_3}{D_2}\right)}, \quad (3)$$

where $d$ and $D$ are diameters of the core and insulation, mm; $D_2$ and $D_3$ are diameters of the defect inner and outer surfaces, mm; $L_1$, $L_2$ are lengths of Sects. 1 and 3; $l_x$ is the defect length (Sect. 2).

Figure 8 shows dependence of the capacitance and relative error on the length of the intrinsic defect in the range from 0 to 5 cm at a fixed defect thickness $h = D_3 - D_2 = 0.4$ mm.

Figure 8 shows that the *Foreign inclusion* defect decreases the capacity. The value of the wire capacitance attains threshold at a length of $l_x = 3$ cm and a fixed defect thickness $h = 0.4$ mm, which is more than 6% of the insulation volume of the defect-free wire.

Figure 9 shows the dependence and relative error of the capacitance on the thickness of the intrinsic defect $h$ in the range from 0 to 0.5 mm at a fixed defect length $l_x = 3$ cm.

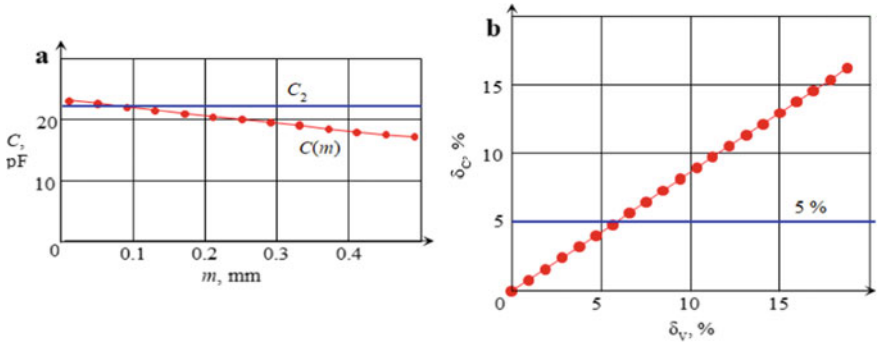


**Fig. 8** Change in wire capacitance **a** and relative error **b** on changes in the length of the intrinsic defect

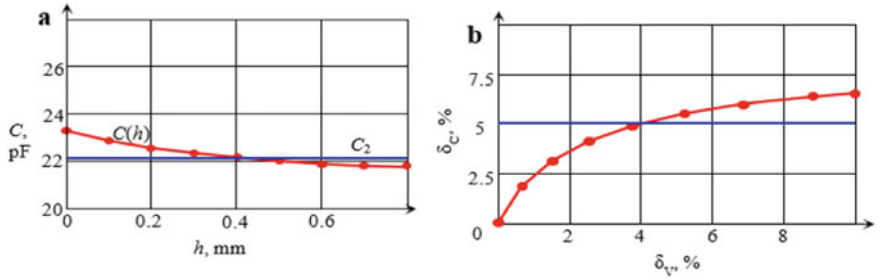


**Fig. 9** Change in wire capacitance **a** and relative error **b** on changes in the thickness of the intrinsic defect

A significant change in the capacitance of the wire is observed when the thickness of the wire defect changes by more than 0.4 mm with a fixed length of the defect $l_x$ = 3 cm (Fig. 9). This type of defect leads to a change in the wire insulation volume by more than 4% of the defect-free wire volume.

## 4 Conclusion

Modeling allows complex studies of the effect of various types of insulation defects on wire capacitance with no significant expenditures for creating a bank of samples.

The paper presents models of the following defects: eccentricity, local insulation thinning and foreign inclusion, which are quite difficult to investigate. In addition, it is almost impossible to provide variability of one of the geometric dimensions while the other one is constant.

The study has shown that defects cause changes in the capacitance. The wire capacitance can significantly change (by 5%) under the following conditions:

- 4.5% increase in the defect volume relative to the total volume of the wire at increased length of the defect, and 3.3% increase at the increased depth of the defect;
- eccentricity of 10% and greater of the core diameter value;
- 6% increase in the volume of the intrinsic defect relative to the total volume of the defect-free wire at increased length of the defect and 4% increase at increased thickness of the defect.

This study presents simplified models of defects since it is only the first stage of the research. Further research will focus on improving the reliability of the models. In addition, the effect of other types of defects and their geometric dimensions on wire capacitance will be investigated to show the possibility of detecting various types of defects during technological testing of wire capacitance.

## References

1. Murty, P.S.R: Cables. In: Electrical Power Systems (Chap. 7), pp. 145–169 (2017). https://doi.org/10.1016/B978-0-08-101124-9.00007-3
2. Bryant, R.: Irradiation of cables, wires and heat shrinkables. Radiat. Phys. Chem. **174**, 108895 (2020). https://doi.org/10.1016/j.radphyschem.2020.108895
3. Furse, C., Haupt, R.: Down to the wire. IEEE Spectr. **38**(2), 35–39 (2001)
4. Wenbin, S., Ju, T., Cheng, P., Guodong, M., et al.: Improvement of insulation defect identification for DC XLPE cable by considering PD aging. Int. J. Electr. Power Energy Syst. **114**, 105409 (2020). https://doi.org/10.1016/j.ijepes.2019.105409
5. Drobny, J.G.: Polymers for Electricity and Electronics: Materials, Properties, and Applications. Wiley, New York (2012)

6. Ilie, S., Setnescu, R., Lungulescu, E.M., et al.: Investigations of a mechanically failed cable insulation used in indoor conditions. Polym. Test. **30**(2), 173–182 (2011). https://doi.org/10.1016/j.polymertesting.2010.11.016
7. Vavilova, G.V., Ryumkin, A.V.: Detection of insulation defects in the wire through measuring changes in its capacitance. IOP Conf. Ser.: Mater. Sci. Eng. **289**, 012017 (2018). https://doi.org/10.1088/1757-899X/289/1/012017
8. Jeon, J.C., Kim, J.-J., Choi, M.I., et al.: Detection and location of cable fault using improved SSTDR. Trans. Korean Inst. Electr. Eng. **65**(9), 1583–1589 (2016). https://doi.org/10.5370/KIEE.2016.65.9.1583
9. Severengiz, M.: Challenges and approaches for a continuous cable production. Proc. CIRP **40**, 18–23 (2016). https://doi.org/10.1016/j.procir.2016.01.040
10. Goldshtein, A.E., Vavilova, G.V., Mazikov, S.V.: Capacitance control on the wire production line. MATEC Web Conf. **79**, 01009 (2016). https://doi.org/10.1051/matecconf/20167901009
11. Paulter, N.G.: An assessment on the accuracy of time-domain reflectometry for measuring the characteristic impedance of transmission lines. IEEE Trans. Instrum. Meas. **50**(5), 1381–1388 (2017). https://doi.org/10.1109/19.963214
12. Kapranov, B.I., Vavilova, G.V., Volchkova, A.V., et al.: Mathematical modeling of tomographic scanning of cylindrically shaped test objects. IOP Conf. Ser.: Mater. Sci. Eng. **363**, 012015 (2018). https://doi.org/10.1088/1757-899X/363/1/012015
13. Kosar, V., Gomzi, Z.: Modeling of the power cable production line. Thermochim. Acta. **457**(1–2), 70–82 (2007). https://doi.org/10.1016/j.tca.2007.02.020
14. Abboud, L., Cozza, A., Pichon, L.: A matched-pulse approach for soft-fault detection in complex wire networks. IEEE Trans. Instrum. Meas. **61**(1), 1719–1732 (2012). https://doi.org/10.1109/TIM.2012.2187246
15. Surzhikov, A.P., Pritulov, A.M., Lysenko, E.N., et al.: Calorimetric investigation of radiation-thermal synthesized lithium pentaferrite. J. Therm. Anal. Calorim. **101**(1), 11–13 (2010). https://doi.org/10.1007/s10973-010-0788-7
16. Doskeyev, G.A., Edenova, O.A., Spivak-Lavrov, F.: Influence of the fringe field on moving of the charged particles in flat and cylindrical capacitors. Nucl. Instrum. Methods Phys. Res., Sect. A **645**(1), 163–167 (2011). https://doi.org/10.1016/j.nima.2011.01.132
17. Ravanamma, R., Muralidhara, R., Venkata, K.K., et al.: Structure and morphology of yttrium doped barium titanate ceramics for multi-layer capacitor applications. Mater. Today Proc. (2020). https://doi.org/10.1016/j.matpr.2020.07.646
18. Pulkkinen, J., Koivo, H.N., Zaramella, J.-C.: Capacitance/Diameter (C/D) Control in telephone cable insulation process. IFAC Proc. **29**(1), 725–729 (1996). https://doi.org/10.1016/S1474-6670(17)57747-2
19. Jing, D., Kang, L., Eileen, H.-J.: Energy monitoring and quality control of a single screw extruder. Appl. Energy **113**, 1775–1785 (2014). https://doi.org/10.1016/j.apenergy.2013.08.084
20. Hansson, S., Fisk, M.: Simulations and measurements of combined induction heating and extrusion processes. Finite Elem. Anal. Des. **46**(10), 905–915 (2010). https://doi.org/10.1016/j.finel.2010.06.004
21. Natheer, A.: Effects of cable insulations' physical and geometrical parameters on sheath transients and insulation losses. Int. J. Electrical Power Energy Systems **110**, 95–106 (2019) https://doi.org/10.1016/j.ijepes.2019.02.047
22. Ayokunle, A., Ademola, A., Lambe, M.A.: Predicting extrusion process parameters in Nigeria cable manufacturing industry using artificial neural network. Res. Article **6**(7), E04289 (2020). https://doi.org/10.1016/j.heliyon.2020.e04289
23. Loete, F., Zhang, Q., Sorine, M.: Experimental evaluation of the inverse scattering method for electrical cable fault diagnosis. IFAC-PapersOnLine **48**(11), 766–771 (2015). https://doi.org/10.1016/j.ifacol.2015.09.619
24. Ulf, B.: Extrusion User's Guide to Plastic (2nd ed., Chap. 20) pp. 177–203 (2019) https://doi.org/10.3139/9781569907351.020

25. Albert, L., Deschamps, F., Jolivet, A., et al.: A current synthesis on the effects of electric and magnetic fields emitted by submarine power cables on invertebrates. Mar. Environ. Res. **159**, 104958 (2020). https://doi.org/10.1016/j.marenvres.2020.104958
26. Halim, H., Phung, B.T., Fletcher, J.: Impact of electromagnetic fields on current ratings and cable systems. In: Proceeding of the 2014 International Conference on Smart Green Technology in Electrical and Information Systems (ICSGTEIS), 1–6 (2014). https://doi.org/10.1109/ICSGTEIS.2014.7038727
27. Kelly, A.L., Brown, E.G., Coates, P.D.: The effect of screw geometry on melt temperature profile in single screw extrusion. Polym. Eng. Sci. **46**(12), 1706–1714 (2003). https://doi.org/10.1002/pen.20657
28. Ballou, G.: Resistors, Capacitors, and Inductors. Handbook for Sound Engineers (4th ed., Chap. 10), pp. 241–272 (2008). https://doi.org/10.1016/B978-0-240-80969-4.50014-6
29. Lysenko, E.N., Surzhikov, A.P., Vlasov, V.A., et al.: Synthesis of substituted lithium ferrites under the pulsed and continuous electron beam heating. Nucl. Instrum. Methods Phys. Res., Sect. B **392**, 1–7 (2017). https://doi.org/10.1016/j.nimb.2016.11.042
30. Spivak-Lavrov, I.: Chapter two-analytical methods for the calculation and simulation of new schemes of static and time-of-flight mass spectrometers. Adv. Imag. Electron Phys. **193**, 45–128 (2016). https://doi.org/10.1016/bs.aiep.2015.10.001
31. Nizhegorodov, A.I., Bryanskikh, T.B., Gavrilin, A.N., et al: Testing a new alternative electric furnace for vermiculite concentrates heat treatment. Bulletin of the Tomsk Polytechnic University. Geo Assets Eng. **329**(4), 142–153 (2018)